

Simulation of the free energy of mixing for blend components in a new family of flexible polycyanurates

Ian Hamerton*, Brendan J. Howlin, C. Robert Pratt

Chemical Sciences Division, Faculty of Health and Molecular Sciences, University of Surrey, Guildford, Surrey GU2 7XH, UK

ARTICLE INFO

Article history:

Received 22 July 2010

Received in revised form

24 September 2010

Accepted 27 September 2010

Available online 21 October 2010

Keywords:

Cyanate esters

Polycyanurates

Blends

ABSTRACT

The miscibility of the dicyanate of bisphenol A, with three dicyanate monomers, with aryl/alkylene ether backbones is studied at different compositions of a binary blend. Solubility parameters are calculated for dicyanate monomers and selected oligomers using the methods of Small and Fedors to predict compatibility. The results are evaluated in terms of the accuracy of the model in reproducing observed data. Gibbs free energy of mixing (ΔG_{mix}) values for selected blends are calculated using the BLENDS module of Cerius². Empirical data (HPLC and MS) are used to inform the construction of selected models to represent different stages of polymer conversion. DMTA analysis is performed to examine the thermo-mechanical properties of the resulting blends and compared with the simulated blend data.

© 2010 Elsevier Ltd. All rights reserved.

1. Introduction

Cyanate esters can be termed high performance thermosetting polymers, despite having physical and mechanical properties that fall between epoxy resins and BMIs [1] (e.g. glass transition temperatures, T_g , of between 200 and 300 °C depending on structure and degree of cure) although the very low moisture absorption values that they exhibit are superior to both competitor resins (e.g. this may be as low as 0.6–2.5 wt% depending on backbone structure, compared with figures of 4–4.5 wt% for BMIs or 3–6 wt% for commercial epoxies) and is backed up by good hot/wet properties. Cured cyanates may find application in a variety of niche technological applications (e.g. microelectronics [2], high performance adhesives and advanced composites). The combination of properties that make them attractive in these areas include good adhesion to a variety of substrates (e.g. metals, glass and carbon fibres) with values of 14–20 MPa (for lap shear strength) on 2024 T-3 aluminium alloy, which is significantly higher than corresponding aerospace epoxies. Cured polycyanurates also show exceptionally low dielectric constants, $\epsilon = 2.2$ –2.7 and dissipation factors, $D_f = 0.003$ at GHz frequencies, coupled with low loss behaviour, which has ensured the continuing application of cyanates in the fabrication of microelectronics components such as multichip modules and in stealthy coatings and structures [3,4].

Furthermore, the relatively low coefficients of thermal expansion that are exhibited by cured polycyanurates make them of great interest in applications involving multichip modules (MCMs) since the substrate (silicon) has a CTE that is markedly lower than most organic polymers, leading to differential contraction, cure stress and delamination in the final microelectronic package. Commercial cyanate esters are commonly blended or co-reacted with other monomers to modify features such as CTE or fracture toughness and the ability to predict the miscibility behaviour of these blended systems would be of great advantage. Consequently, the object of the present work is to examine the optimum blend of bisphenol A dicyanate (which is the most commonly studied commercial monomer) with a series of three aryl dicyanates with alkylene ether backbones of varying backbone length over a range of temperatures (the latter have been previously reported elsewhere [5]).

The aim of this work is to develop a robust method to predict the miscibility behaviour of either co-monomers (in this case using different dicyanate monomers) or to predict the behaviour of monomer/oligomer blends. This would potentially be of use in understanding when e.g. phase separation occurs and how this might influence fracture toughness in cyanate ester blends. In this preliminary study, binary blends were studied comprising a commercial dicyanate and selected newly-synthesized dicyanates with alkylene backbones for which interesting thermo-mechanical properties have been observed. We report the miscibility calculated for the co-monomers and also for the binary blends during the early stages of polymerisation.

* Corresponding author. Tel.: +44 1483 689587; fax: +44 1483 686851.

E-mail address: i.hamerton@surrey.ac.uk (I. Hamerton).

2. Experimental section

2.1. Formulation of monomer/co-catalyst blends

A series of general methods were employed to produce three different cyanate ester monomers, differing only in the bridging chain length (*i.e.* the value of *n*). Consequently, the preparative procedure and characterisation data for compounds **1**, **2**, **3**, and **4** have already been reported in detail [5]. Prior to incorporation in the dicyanates, the co-catalyst package, comprising Al(acac)₃ and dodecylphenol in the molar ratio of 1:25, were first homogenised by heating to 80 °C (in a vial in a water bath) before cooling to room temperature. The co-catalysts were then introduced into the dicyanate monomers by mixing in a pestle and mortar at room temperature to a homogeneous mixture. The newly-prepared dicyanates **4a**, **4b** and **4c** were then added to samples of bisphenol A dicyanate, each at a ratio of 20:80 wt% and cured according to the schedule described in Section 2.2.

2.2. Cure schedule for the monomer/co-catalyst blends

A glass slide was placed and clipped over a glass slide-covered high temperature silicone adhesive slide with a pre-cut PTFE template of dimensions 35 × 10 × 1 mm³, and heated in an oven to 230 °C to remove residual solvent in the adhesive. This ensured that the PTFE adhered to the glass. The prepared moulds were placed on a pre-heated hot plate at 90 °C for **4a**, at 80 °C for **4b** and at 60 °C for **4c**. Each blend was placed in one of these templates and allowed to become molten, sufficient sample was added to cover the entire volume of the template. The monomers and blends were heated as neat melts to ensure that voids did not occur during the cure process due to trapped air or solvents released, as this can be harmful to the properties of the polymer. The molten monomers and blends were then transferred to a vented oven under air and cured at 180 °C/1 h and finally at 230 °C/1 h. The cure schedule is relatively mild to compensate for the presence of the alkylene ether dicyanates because in preliminary studies, using a common commercial cure schedule¹, the homopolymers of **4a**, **4b** and **4c** produced very dark polymers, suggesting charring. There is no suggestion that this cure schedule is optimised for either of the monomers.

2.3. DMTA apparatus

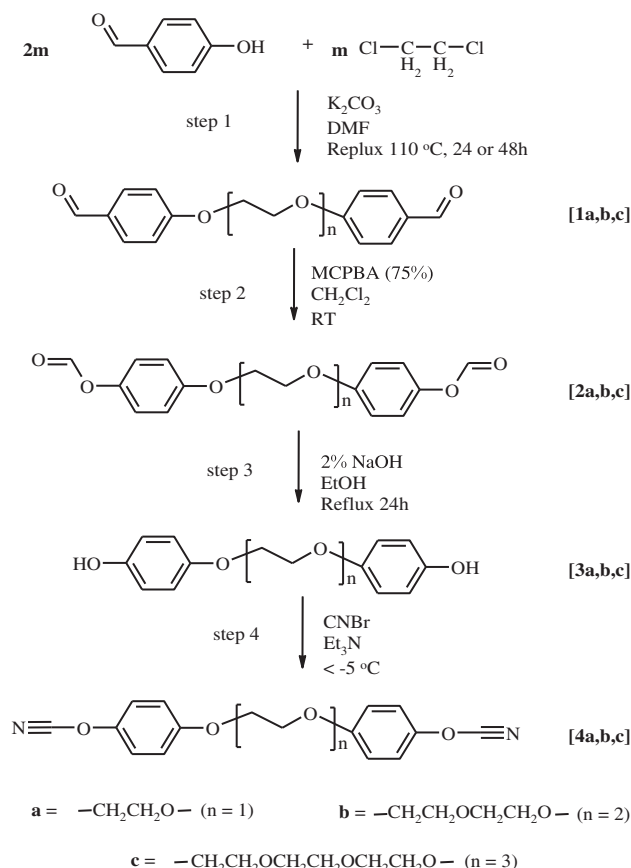
Dynamic mechanical thermal analysis (DMTA) measurements for the polymers were undertaken in dual cantilever bending mode on cured neat resin and blend samples (10 × 30 × 1 mm³) using a Polymer Laboratories Dynamic Mechanical Thermal Analyser with a Polymer Laboratories environmental controller unit. Temperature scans were performed between –150 and 300 °C at 5 K min^{–1} at a frequency of 1 Hz.

2.4. Simulation apparatus

The molecular simulations were conducted using a Silicon Graphics Machine single R4k, 64 MB RAM and a video card using the IRIX 6.4 operating system. Molecular mechanics simulations were performed within Cerius² (Molecular Simulations, Inc.).

2.5. Construction of the molecular models

Initially, a model of the homopolymer of bisphenol A dicyanate was constructed using the builder module within Cerius² to test the methodology as extensive studies have been undertaken previously on this polymer using similar techniques [6,7]. The bond lengths and angles within the bisphenyl moieties were based on data collected using single crystal X-ray crystallography experiments [8]. Partial Charges calculated using equivalent charges [9] and the molecular structures initially minimised using the Dreiding II forcefield [10] followed by a modified forcefield previously developed within our group [11] to incorporate an additional parameter set specifically designed to accommodate the triazine ring. The polymerisation of dicyanate monomers proceeds *via* a cyclotrimerisation mechanism [12–14] to yield a polycyanurate (based on oxygen-linked *s*-triazine rings) and so molecular units comprising triazine rings with a missing ‘arm’ and one of units remaining unreacted. A series of partially converted polycyanurates ranging from the initial cyclotrimer (*i.e.* *n* = 3) to the nonomer (*n* = 9) was constructed and a conformational study was carried out on the cyclotrimer of bisphenol A dicyanate A and the final structures were saved to file. The amorphous builder module of Cerius² was then used to create repeating cells and the ‘head’ and ‘tail’ units had to be adjusted manually so that they connected *via* covalent bonds. Initially, this created a crystalline structure, but as the true polycyanurate is amorphous a molecular dynamics (MD) simulation was performed to remove the inherent anisotropy in the system. The density was calculated using molecular mechanics (MM) and compared to densities determined experimentally [15]. The blended model was constructed to yield a largely random distribution of the two selected components.



Scheme 1. Synthetic route to the dicyanate monomers (**4a**, **4b**, **4c**).

¹ A typical casting procedure for cyanate ester resins incorporating zinc naphthenate (60–150 ppm metal) and nonyl phenol (2 ph) involves a gelling step (104–150 °C), followed by curing at 177 °C (1 h) + 210 °C (1 h) and a free-standing post cure at 250 °C (2 h).

Table 1
Small solubility parameter δ_H for monomers and polymers.

	δ_H (MPa ^{1/2})	
	Monomer	Polymer
Bisphenol A dicyanate	25.20	26.69
4a	26.24	28.11
4b	25.29	26.85
4c	24.57	25.91

2.6. Calculation of the binary blends

Initially, BLENDS was tested with monomers of bisphenol A dicyanate and **4a–c**, with the expectation that they would be miscible and that favourable energies of mixing would be returned. The BLENDS module was initially trialled employing 10,000 interaction energies, but this was revised to 500 after only 200 interactions had been determined after 5 min 25 Trials per cluster were attempted for 25 different clusters for each interaction pair. This was revised downwards from the default value of 100, again due to time constraints. Values of A, B and C were obtained for the Kamide analytical fit function and the Gibbs free energy of mixing was then calculated. Free energies were calculated for a range of temperatures and volume fractions and these compared well with the interactions produced by analysis of the results in Cerius².

2.7. Selection of parameters

Since the variables used were arbitrarily chosen values for time convenience rather than accuracy of calculation they were checked by an extensive run. The calculation was repeated with 2000 interaction energies determined and 100 clusters were utilised for determination of coordination number. It was suspected that little difference would be found for small units, as the real-time graphs generated by BLENDS converged within the initial parameter set.

3. Results and discussion

The original choice for an examination of the alkylene ether backbone moiety was prompted by previous work [16] to examine the properties of another family of thermosetting polymers (BMIs) for which brittleness can also be a drawback. Following extensive work, a series of reported synthetic steps were combined to produce the four step reaction pathway shown in Scheme 1 to produce three novel dicyanate monomers [5,15] and the same numbering scheme has been retained to identify these compounds (**4a**, **4b**, **4c**), having

similar alkylene ether backbone structures that differ in length and generically identified by $n = 1, 2, 3$ to denote the number of ethoxy segments in the chain.

The choice of the dicyanate based on bisphenol A as the second component in the blends was based on the extensive research literature available for direct comparison.

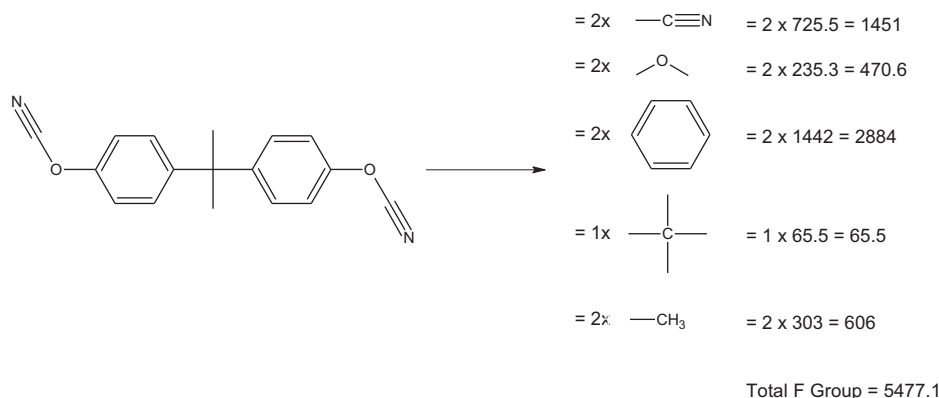
3.1. Initial miscibility studies based on Fedors' method

Initially the study focused on the early stages of polymerisation; the later stages of the reaction are less relevant, particularly after the gel point has been passed as steric effects tend to dominate network formation [12], making miscibility less important. Thus, the main focus of the study was the affinity of monomeric and oligomeric molecules with each other. A rapid method of estimating the co-miscibility of molecules involves the calculation of solubility parameters and while this is not the most accurate method it does provides a somewhat "rough and ready" solution. Consequently, before commencing on the empirical study solubility parameters were estimated for monomers and higher weight polymeric units, using a calculation reported by Fedors [17] (and based on the Hoy solubility parameter [18]), $\delta_H = (\Delta E_v/V)^{1/2}$ using a simple single temperature (25 °C) method where,

$$\delta_H = \left[\frac{\sum_i \Delta e_i}{\sum_i \Delta v_i} \right]^{1/2} \quad (1)$$

(Δe_i and Δv_i are the additive atomic group contributions for the energy of vaporisation and the molar volume respectively at a given temperature). This additive method produces a calculated solubility parameter, δ_H , which depends on the nature of functional groups/moieties within the monomer/polymer blend structure(s). On this basis, δ_H was calculated for the dicyanate monomers and polycyanurates giving the values in Table 1 below, where if the calculated values of δ_H for the two components are similar, then they will be compatible. This simple method should only be taken as an initial guide to the ambient temperature compatibility of the components of the blend. It was not intended to determine the dynamics of the mixing of the components during the cure, which may be influenced by a number of factors and may lead to a complex phase diagram.

Comparing the values given in Table 1, one would expect each of the synthesised monomers to be compatible with the monomer of bisphenol A dicyanate and indeed with each other. Commercial prepolymers of bisphenol A dicyanate, notionally containing a larger proportion (ca. 30%) of triazine rings, should be more



Scheme 2. Calculation of F group contributions ((MPa)^{1/2} cm³ mol^{−1}) based on structural fragments.

Table 2

Selected solubility parameters calculated using various methods.

Group	Small	Hoy	
	$F \text{ (MPa)}^{1/2} \text{ cm}^3 \text{ mol}^{-1}$	e_i	v_i
<i>p</i> -phenylene	1442	7630	71.4
C(–)4	65.5	350	–19.2
–CH ₃	303	1125	33.5
>CH ₂	269	1180	16.1
–O–	235.3	800	3.8
CN	725.5	6100	24
Triazine	1000	8000	52.4

compatible with **4a**, as δ_H would be higher than that of the bisphenol A dicyanate monomer. The preliminary calculations of solubility (using the Fedors' solubility parameter, δ_H) suggested that of the monomers studied, the values of bisphenol A dicyanate and **4b** were closest in magnitude (with a difference of $0.09 \text{ MPa}^{1/2}$, Table 1) and thus should produce the most compatible blend. In contrast, and by the same token, the binary blend of bisphenol A dicyanate and **4a** should form the least compatible monomer blend (with a difference of $1.04 \text{ MPa}^{1/2}$). Thus, the calculation suggests the following order of compatibility of bisphenol A dicyanate ($> =$ more soluble than) **4b** > **4c** > **4a**, although this absolute order was not entirely borne out by the empirical observations.

3.2. Initial miscibility studies based on Small's method

In the current study, this somewhat simplistic method was extended to incorporate the Small solubility parameters [19], and Flory–Huggins theory in order to predict miscibility based on the

density of compounds and the nature of their functional groups. Thus, the Small equation was used:

$$\delta = \frac{\sum F}{V} = \frac{(\sum F)\rho}{M} \quad (2)$$

where δ = solubility parameter F = molar attraction constant ρ = density M = molecular mass V = molecular volume

Molecules with similar solubility parameters are likely to be miscible and, when combining two co-monomers, statistical copolymer networks will form where the two monomers are mutually compatible. Where the monomers are immiscible block polymerisation is more likely, resulting in unpredictable, heterogeneous characteristics across the material. If this is the case the network formation will be driven by statistical rules, *i.e.* there is a roughly equal chance of a monomer of A and B undergoing reaction. A trial was first performed on a monomer of bisphenol A dicyanate and the solubility parameters (*i.e.* total F group contributions) were calculated (Scheme 2) from a table of published values [20,21].

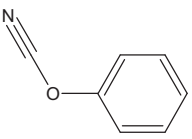

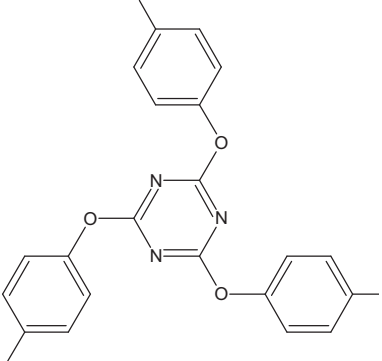
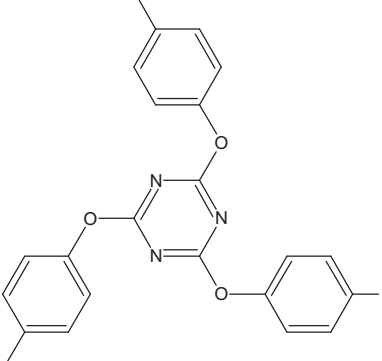
Solubility parameters are based on molecular group contributions and inevitably not all molecular groups are accounted for in the tables listed.

3.3. Comparison of group contribution methods

Solubility parameters were calculated using both Fedors' and Small's methods, taking repeat units in oligomeric structures and summing fractional contributions (Table 2). These values were obtained for all sub-units of the structures apart from the *s*-triazine ring (which was absent from the literature tables). Thus, a value was

Table 3

Selected group contributions.

Group Code	Structure	Small	Fedors	
		$F \text{ (MPa)}^{1/2} \text{ cm}^3 \text{ mol}^{-1}$	e_i	v_i
A		2402.8	–	–
B		671.5	14530	99.2
C _{n=1}		1008.6	2600	47.8
C _{n=2}		1781.9	3960	39.8
C _{n=3}		2555.2	7120	75.8
D		3328.5	10280	111.8

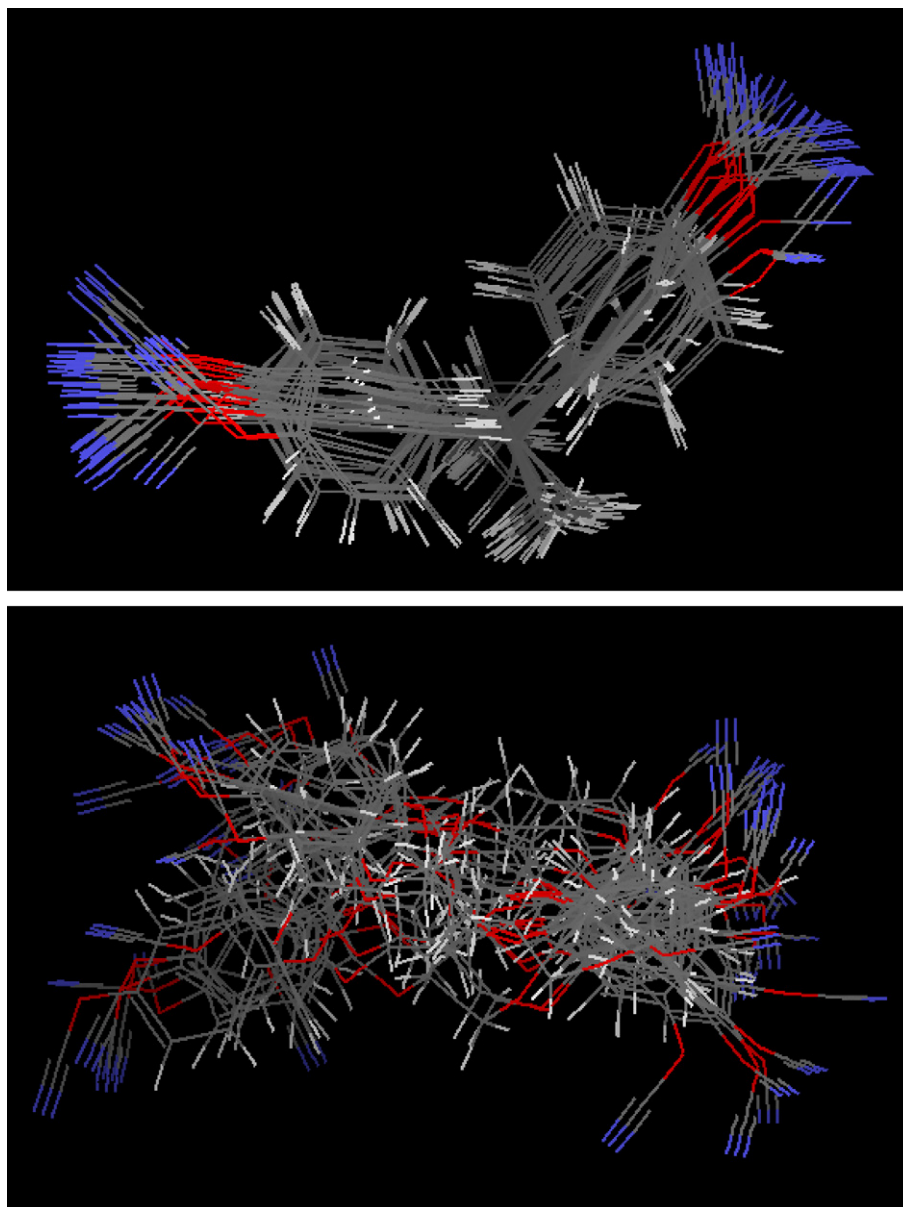


Fig. 1. Conformational Analysis of monomers of bisphenol A dicyanate (top) and **4a** (bottom).

estimated using values taken from a substituted phenyl ring and three cyanate groups which when rounded up produced a figure close to that for a phenyl group.

Calculating the values for each unit of interest, *e.g.* bisphenol A dicyanate monomer, trimer, pentamer, alkylene ether monomer, *etc.* proved somewhat time consuming and so a general method was created in which all the structures were broken down into common sub-units whose group contributions were then calculated (Table 3). The number of each subunit was counted for each molecule and the total F group contributions were determined from this. The molar masses and densities were calculated in ChemSketch (Advanced Chemistry Development, Inc., 110 Yonge Street, 14th floor, Toronto, Ontario, Canada M5C 1T4, <http://www.acdlabs.com/home/>) and the solubility parameter was then evaluated with an Excel function; the value obtained was then compared to one calculated previously and, as a measure of internal consistency; the calculated densities were subsequently validated using empirical data [15].

3.4. Miscibility studies using Cerius²

A matrix for various mixture combinations was proposed on the basis of obtaining a representative sampling of chemical space (*i.e.* the interactions for a given monomer with its corresponding trimer, pentamer and so on). This produced a large number of calculations (276), which were submitted in the batch mode of Cerius². The polymerisation of dicyanate monomers proceeds *via* a cyclotrimerisation mechanism [22,23] to yield a polycyanurate (based on *s*-triazine rings) and so molecular units comprised triazine rings with a missing 'arm' and one of the units remaining unreacted. A series of partially converted polycyanurates ranging from the initial cyclotrimer (*i.e.* $n = 3$) to the nonomer ($n = 9$) was constructed and a conformational study was carried out on the cyclotrimer of bisphenol A dicyanate. It was noted that the structures generated only remained in feasible conformations for a static time shot (in the case of bisphenol A dicyanate it was thought that the structures were representative as there is little rotational freedom about the central

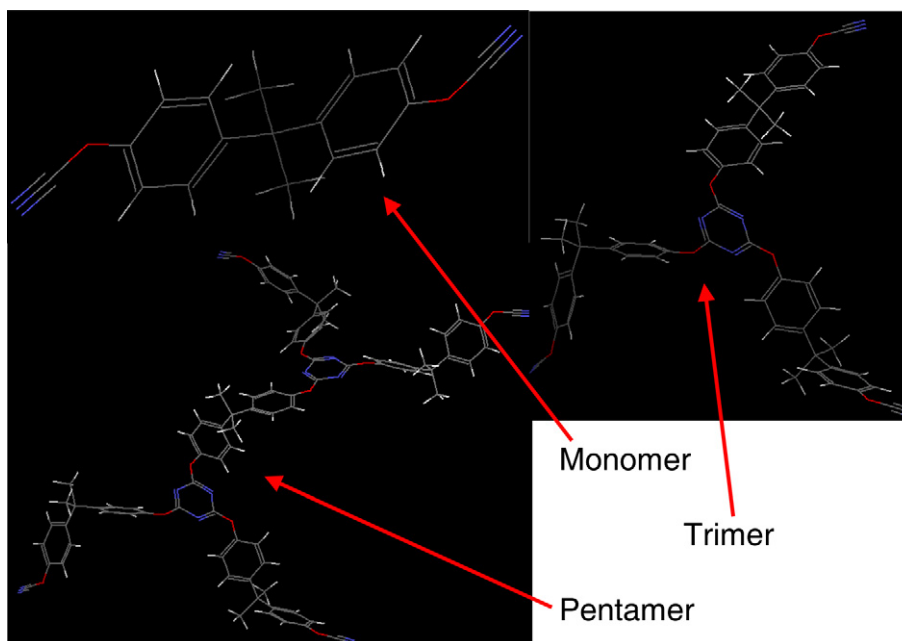


Fig. 2. Structures of Bisphenol A dicyanate monomer, trimer and pentamer.

group [24]). For the novel modifier series the number of rotatable bonds was somewhat higher and the number of possible conformations might have a significant effect on the network structure and make it more difficult to generate representative structures. To gauge this effect a conformational analysis of monomers of bisphenol A dicyanate and **4a** was undertaken and torsion angles in each structure were identified by a search for rotatable bonds, ring flex was excluded from the search. Six torsion angles were identified for bisphenol A dicyanate and nine for **4a**. Boltzmann jump searches were then carried out to generate 25 conformers by simulated heating of the molecules. The files were then processed (the conformers were generated as unique structures) and the 25 structures were overlaid using a RMS minimised volume overlay. The variation in structures was determined from this overlay (Fig. 1).

From which the molecular flexibility and hence conformational freedom imparted by the central bridge is immediately apparent. The bisphenol A dicyanate structures for the monomer, trimer and pentamer built in Cerius² are given below (Fig. 2) and they reveal the 3D nature of the network as it forms.

Bond lengths and angles for the cyclotrimers from the MM experiments are in good agreement with previously published values [11] (C–N distances for the *s*-triazine ring ranges from 1.343–1.352 Å; C–N–C angles 119.96–120.42°; N–C–N angles 119.46–120.04°), demonstrating that the modified forcefield reproduced the bond geometries accurately. The amorphous builder module of Cerius² was then used to create repeating cells and the ‘head’ and ‘tail’ units had to be adjusted manually so that they connected. This created a crystalline structure, but as the true polycyanurate is amorphous a molecular

Table 4

Total molar attraction constants for selected compositions based on network growth for different dicyanates.

Fragment	Composition							Solubility Parameters (MPa ^{1/2}) cm ³ mol ⁻¹	
	A	B	C _n = 0	C _n = 1	C _n = 2	C _n = 3	D	Hoy	Small
Monomer BisA	2	1	0	0	0	0	0	11.34	23.05
Monomer <i>n</i> = 0	2	0	1	0	0	0	0	11.77	24.94
Monomer 4a	2	0	0	1	0	0	0	11.49	24.16
Monomer 4b	2	0	0	0	1	0	0	11.26	23.59
Monomer 4c	2	0	0	0	0	1	0	11.08	23.14
Trimer BisA	3	3	0	0	0	0	1	10.85	22.66
Pentamer BisA	4	5	0	0	0	0	2	10.75	22.58
Heptamer BisA	5	7	0	0	0	0	3	10.70	22.55
Trimer <i>n</i> = 0	3	0	3	0	0	0	1	11.30	24.65
Trimer 4a	3	0	0	3	0	0	1	11.06	24.52
Trimer 4b	3	0	0	0	3	0	1	10.87	24.42
Trimer 4c	3	0	0	0	0	3	1	10.72	24.34
Pentamer <i>n</i> = 0	4	0	5	0	0	0	2	11.20	24.58
Pentamer 4a	4	0	0	5	0	0	2	10.97	24.50
Pentamer 4b	4	0	0	0	5	0	2	10.79	24.43
Pentamer 4c	4	0	0	0	0	5	2	10.65	24.38
Heptamer <i>n</i> = 0	5	0	7	0	0	0	3	11.16	24.55
Heptamer 4a	5	0	0	7	0	0	3	10.93	24.49
Heptamer 4b	5	0	0	0	7	0	3	10.76	24.44
Heptamer 4c	5	0	0	0	0	7	3	10.62	24.40

Key: C_n = structures relating to monomers comprising *n* alkylene ether units in backbone (e.g. C_n = 1: oligomeric structures based on **4a**), BisA = bisphenol A dicyanate.

dynamics (MD) simulation was performed to remove the inherent anisotropy in the system. The density was calculated using molecular mechanics and compared to densities determined experimentally [15]. The blended model was constructed to yield a largely random distribution of the two selected components.

3.5. Initial estimations of monomer miscibility using the methods of Hoy and Small

The numbers of each fragment in every monomer-heptamer sized molecule was then counted and the total F group contributions were calculated to yield the following results (Table 4) for a series of growing networks based on different dicyanate monomer blends. A cursory examination of the table indicates that the miscibility of all units is relatively similar and unlikely to become immiscible under normal conditions. A graphical analysis of the data provides a more detailed insight: Fig. 3 shows the variation in the solubility parameter calculated using the Small method as network growth occurs. Notably, higher values for the solubility parameter are calculated for the alkylene ether dicyanate monomers than the bisphenol A dicyanate monomer; the values converge as the number of methylene groups in the backbone increases (so that the values for the bisphenol A dicyanate and **4c** are almost identical). Values calculated for the dicyanate of *bis*(4-hydroxyphenyl)ether are also included for comparison and these are markedly greater than bisphenol A dicyanate, indicating that these monomers would be of lower compatibility. The Small calculation suggests that as the polymerisation proceeds the alkylene ether dicyanates (and *bis*(4-cyanatophenyl)ether) become increasingly similar, but markedly less compatible with the bisphenol A polycyanurate.

Fig. 4 shows the same for Hoy's method. Immediately, the differences in the values from those calculated using the Small method are apparent – the values for the monomers are ranged in a similar order (although the bisphenol A dicyanate monomer now lies above **4b** and **4c**). As the polymerisation proceeds, all solubility parameters fall as network growth occurs, but still differ by a similar amount. There appears to be a reversal in solubility for **4b** and bisphenol A dicyanate as the cyclotrimer first forms. Values calculated for the dicyanate of *bis*(4-hydroxyphenyl)ether are once again the highest of those calculated. The apparent discrepancy in the two calculated behaviours are probably due to the inaccuracy of Hoy's method (i.e. that the implicit assumptions made are relatively

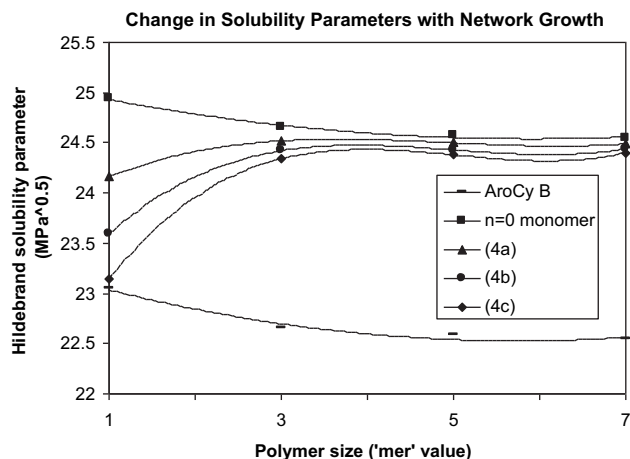


Fig. 3. Variation in solubility parameters ($\text{MPa}^{1/2}$) for different monomers calculated using Small's method as a function of monomer. (polymer size relates to degree of conversion). N.B., AroCy B10 represents bisphenol A dicyanate.

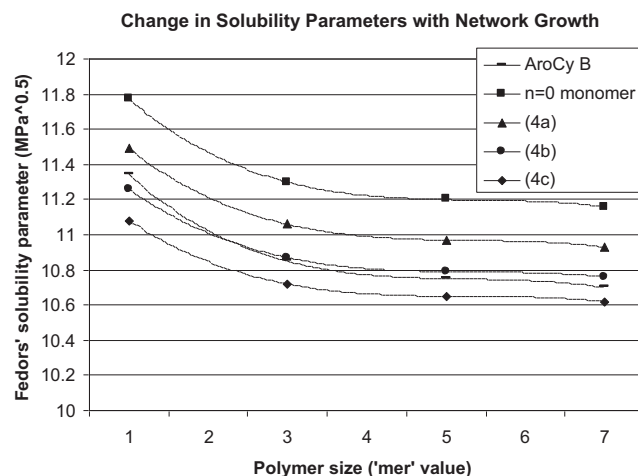


Fig. 4. Variation in solubility parameters ($\text{MPa}^{1/2}$) for different monomers calculated using Hoy's method as a function of monomer. (polymer size relates to degree of conversion). N.B., AroCy B10 represents bisphenol A dicyanate.

simplistic) and prompted a third line of enquiry namely using molecular simulation.

The third graph (Fig. 5) shows the effect of network growth on the solubility parameter calculated using Hoy's method for the alkylene ether dicyanates and *bis*(4-cyanatophenyl)ether. As the alkylene ether chain increases, the solubility parameter falls for each stage of the polycyanurate. This suggests that any slight preference may result initially in monomers reacting together in preference to reacting with trimers or other oligomers (this is consistent with the HPLC data discussed subsequently, in which high initial concentrations of trimer units are found from the reaction of monomers).

The high degree of similarity in solubility parameters is predictable given both Fedors' and Small's use of additive group functions and the inherent similarity in the structural motifs of the monomers (bearing common sub-units). The estimations of density using ChemSketch is an area for possible discrepancies to arise, but once again this uses atom- and group-based calculations and so any deviation from empirically determined densities will be uniform across the structures. The considerations make quantifiable comparisons less rigorous but do allow for relative comparisons to be made between structures.

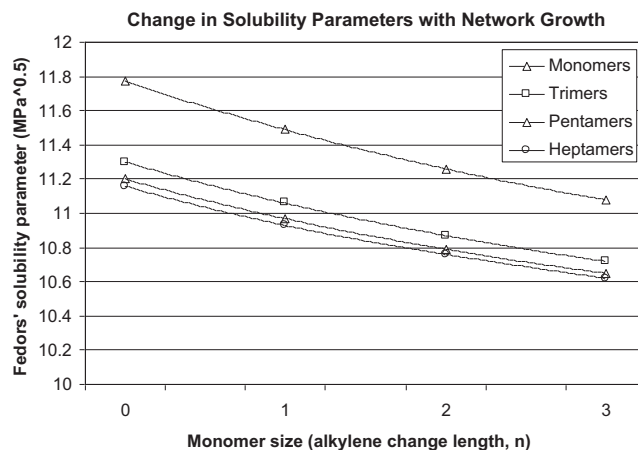


Fig. 5. Variation in solubility parameters ($\text{MPa}^{1/2}$) for different monomeric and oligomeric species calculated using Fedors' method as a function of (polymer size relates to alkylene chain length).

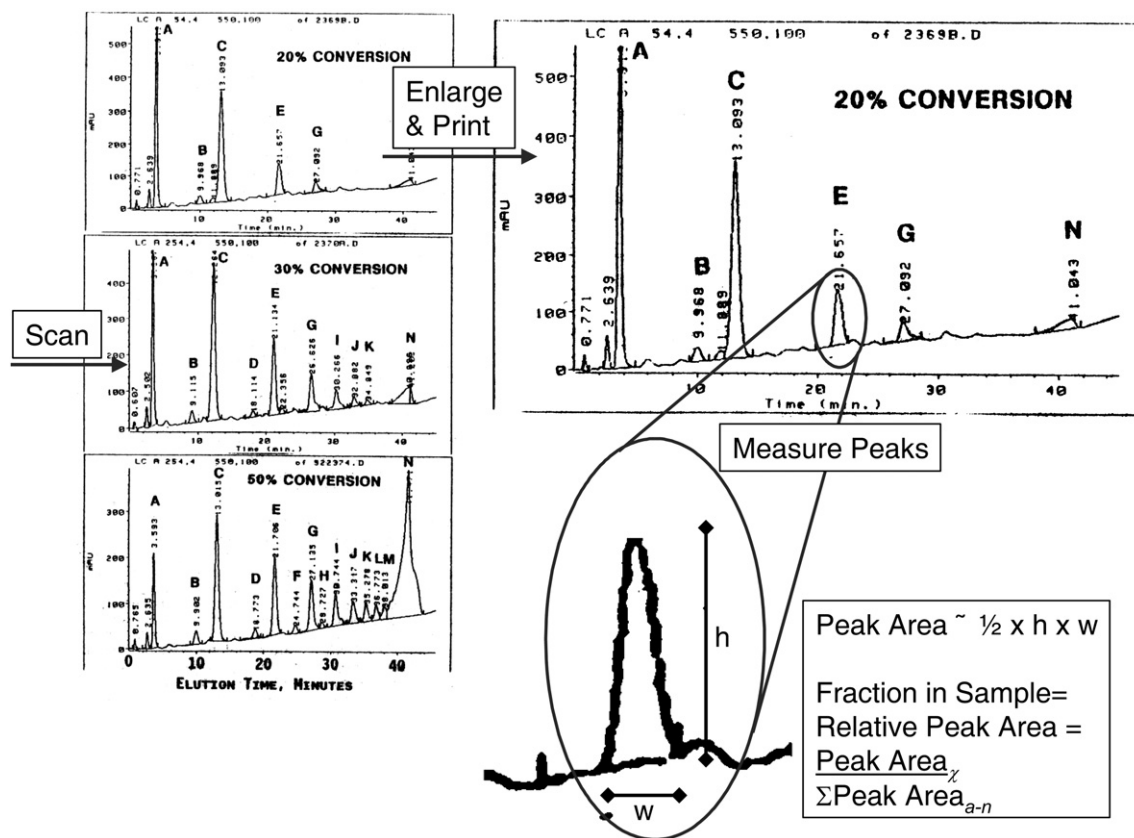


Fig. 6. Schematic showing the treatment of published data to obtain information about the composition of the growing polycyanurate network (data shown originally published in ref. [24]).

3.6. Examination of the growth of the polycyanurate network

The polymerisation of dicyanate monomers has already been described as a series of successive cyclotrimerisation reactions, but this is a simplistic representation for a complex process [25] and historically the actual mechanism of network growth was not well understood (*i.e.* whether reactions occurred preferentially between monomers and monomers or trimers and monomers, *etc.*). However, Shimp carried out an empirical study [26] of network growth in bisphenol A dicyanate to its corresponding polycyanurate using infrared spectroscopy to monitor the kinetics of polymerisation (based on consumption of cyanate groups). At nominal conversions of 20%, 30% and 50% the reaction mixture was quenched and HPLC was employed to detect and separate discrete oligomers up to 15 monomers in size (the nature of each peak was confirmed using secondary ion mass spectrometry). From the HPLC chromatograms it was possible to quantify the amount of each oligomer present, and this highlighted the important interactions at each stage of the polymerisation process. For this work, raw data were obtained from Shimp's article [26], although in order to quantify the data the relevant figures were scanned (Fig. 6) and the peak areas used to give a relative value for the amount of each oligomer present². The process was performed for 20%, 30% and 50% conversion rates and Table 5 shows the key species thought to be present in the growing network.

² At the time of this work being carried out, David Shimp had retired from his position and the original company (HiTek Polymers) had since been acquired by not only Rhone-Poulenc but subsequently Ciba-Geigy and the original data were therefore no longer directly available.

From these data it was possible to determine which species predominated in the polymerisation process, and hence which would be studied within the mixing experiments. The key interactions (*i.e.* between those species) were deduced from plots of the change in composition *versus* conversion. Based on the assumption that a miscible blend would behave in a similar fashion to pure bisphenol A dicyanate it was decided that the key interactions were: monomer-cyclotrimer, monomer-pentamer, monomer-heptamer, and monomer-polymer. The data suggested that from an initial composition composed entirely of dicyanate monomer, after the polymerisation commenced cyclotrimeric units formed quickly, this is consistent with published data [12].

Table 5

Composition of the growing network based on previously published HPLC data.

Peak	Species responsible for peak	% Conversion		
		20	30	50
		Molar fraction in sample		
A	Monomer	0.42	0.25	0.05
B	Bicyclopentane cage structure	0.01	0.02	0.01
C	Cyclotrimer	0.39	0.49	0.14
D	Unknown Species	0	0.01	0.01
E	Pentamer	0.08	0.02	0.08
F	Unknown Species	< 0.01	<0.01	<0.01
G	Heptamer	0.02	0.07	0.05
H	Unknown Species	< 0.01	<0.01	<0.01
I	Nonamer	0	0.03	0.03
J	Undecamer	0	0.01	0.02
K	Tridecamer	0	0.01	0.02
L	Pentadecamer	0	0	0.01
M	heptadecamer	0	0	0.01
N	higher oligomers ($n > 17$)	0.08	0.14	0.58

N.B., peak designations refer to original published data ref. [24].

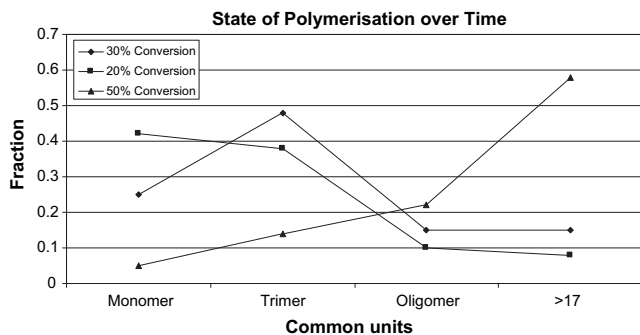


Fig. 7. Major species identified in the growing bisphenol A polycyanurate network at three selected conversions (based on HPLC data originally published in ref. [24]).

The amount of more highly converted material, *e.g.* pentamer to polymer ($n > 17$), was low at the early stages (~ 0.2 at 20%), but rose steadily to ~ 0.3 at 30%. At critical concentrations of cyclotrimer, where the majority of monomer has been consumed (somewhere between 30% and 50% conversion), the cyclic species reacted rapidly to form higher weight fractions. This interpretation suggested that monomer–monomer interactions were very important in the early stages of reaction, trimer–trimer interactions then became more critical and as this progressed the oligomer–oligomer interactions became dominant just prior to the overwhelming influence of steric effects of a highly cross-linked 3D network. These findings informed the identification of the key interactions, without spending unnecessary calculation time on less important interactions. These empirical HPLC data enabled a reasonably accurate series of compositions to be built up during the early stages of the cyclotrimerisation reaction (Fig. 7) and these informed the subsequent experiments using BLENDS.

3.7. Calculation of free energies of mixing using BLENDS

It would be advantageous to be able to correlate quantitatively the variation in chemical nature, molar fraction and degree of polymerisation and their effects on miscibility. All the methods proposed for estimating solubility parameters make assumptions and therefore it was decided that a more sophisticated approach to

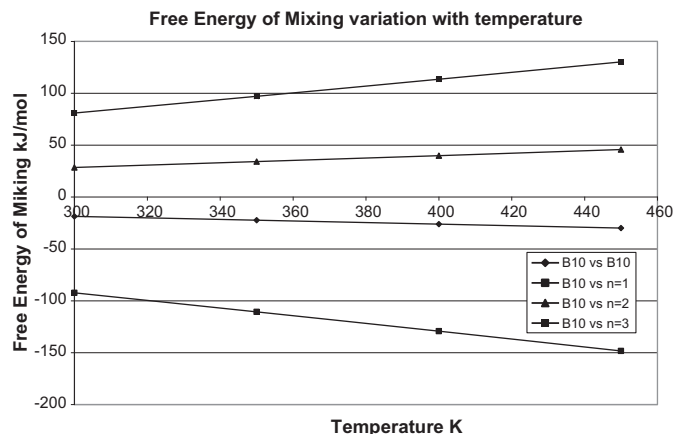


Fig. 9. Temperature Dependence of Gibbs Free Energy of mixing calculated using BLENDS for bisphenol A dicyanate (B10) with alkylene ether dicyanates, $n = 1$ (4a), $n = 2$ (4b), $n = 3$ (4c).

predicting the likely growth was needed. The selected approach was to incorporate miscibility parameters predicted by several methods to calculate free energies of mixing for the different systems over a wide temperature range. The BLENDS calculations in Cerius² allows approximation of solution interaction energies and hence the free energy of mixing [27]. The process is based around the Flory–Huggins model, but extends this by implicitly calculating the coordination number and incorporating temperature dependency by an averaging of interaction energies using the Boltzmann method.

$$\frac{\Delta G}{RT} = \frac{\phi_1}{X_1} \ln \phi_1 + \frac{\phi_2}{X_2} + X(T) \phi_1 \phi_2 \quad (3)$$

where ϕ_x = volume fraction of x and X_x = degree of polymerisation of x .

BLENDS uses two series of measurements to predict free energies: the interaction energies between the species to be mixed and the coordination number, and information on the preference for interaction with like and different species is required for success. The interaction energies, E , are calculated between the two species, E_{12} and E_{21} , and with themselves, E_{11} and E_{22} , by taking a molecule of

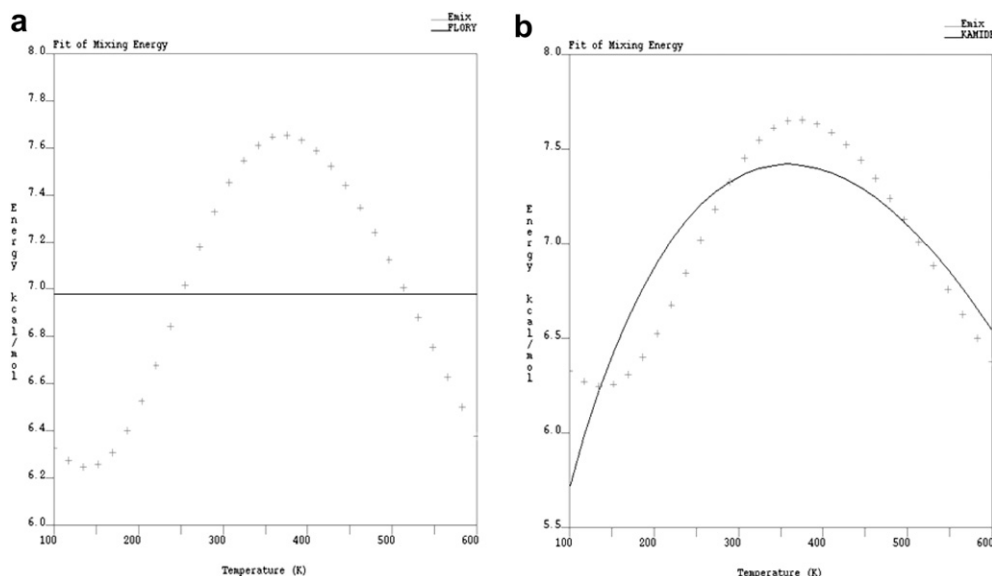


Fig. 8. Representative fits (solid line) for energy of mixing (+) using (a) Flory–Huggins and (b) Kamide models.

Table 6

Temperature dependence of Gibbs free energy calculated using BLENDS.

Binary blend	Temperature (K) value of Gibbs free energy (kJ mol ⁻¹) of mixing			
	300	350	400	450
Bisphenol A dicyanate vs. Bisphenol A dicyanate	-18.67	-22.34	-26.07	-29.87
Bisphenol A dicyanate vs. 4a	-92.39	-110.66	-129.31	-148.30
Bisphenol A dicyanate vs. 4b	28.43	34.10	39.90	45.81
Bisphenol A dicyanate vs. 4c	81.00	97.10	113.53	130.27

the first species and placing it in the centre of the screen; a molecule of the second species is then placed at a position determined by a Monte-Carlo technique to produce a favourable energetic interaction. The process is repeated n times until an average value is obtained; the lower the variance in the data, the more realistic the result. Coordination values (Z) are determined in a similar way, except the interest is now in the number of second species it is possible to fit around the first. Together the product of E and Z values for a given pair of species provides the energetics of that term. Subtraction of the interaction terms for the like molecules from the different pair results in the energy contribution from mixing:

$$X(T) = \frac{E_{\text{mix}}T}{RT} = \frac{(Z_{12}E_{12} + Z_{21}E_{21} - Z_{11}E_{11} - Z_{22}E_{22})}{2RT} \quad (4)$$

The analytical fits used in BLENDS allow for the temperature dependence of X to be accounted for. The values for the Kamide fit (A , B and C) are empirically determined and have no explicit meaning; they are obtained from the interaction terms.

$$X(T) = \frac{(A + BT + CT \ln T)}{RT} \quad (5)$$

Analysis of these calculations can provide temperature, volume fraction and correlated free energies. BLENDS performs these calculations by substituting temperature and molar fraction values into equation (3). E_{mix} and ΔG_{mix} values were determined using the “Analyze” functions in BLENDS. The E_{mix} values are modelled by the aforementioned Flory–Huggins (Fig. 8a) and Kamide (Fig. 8b) fit functions. These illustrate how the temperature dependency of the energy of mixing is accounted for well by the Kamide function, whereas the Flory–Huggins model is less sophisticated and cannot account for it.

Using the BLENDS module it was also possible to calculate phase diagrams for a given blend composition [28], giving an indication of how miscibility would vary over a given temperature range. From a range of mixtures (molar fractions ranging from 0.5:0.5 to 0.8:0.2)

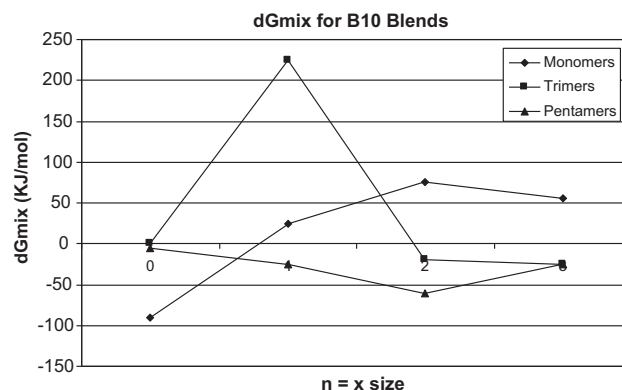


Fig. 11. Effect of backbone length of alkylene ether dicyanates ($n = 1$ (**4a**), $n = 2$ (**4b**), $n = 3$ (**4c**)) on miscibility with similarly-sized bisphenol A dicyanate (B10) species.

it was possible to identify points where systems (involving monomers **4a–4c**) were most likely to result in a statistical copolymer. Fig. 9 demonstrates the temperature and molar fraction dependence of the free energy of mixing is simply obtained from BLENDS and is a powerful illustration of the trends occurring. The example illustrates how it was possible to obtain values for free energy of mixing from structures generated. The values for A, B & C were used to calculate free energies (Table 6). It is apparent that the lowest values of Gibbs' free energy (*i.e.* the best mixing) are calculated for the interaction between bisphenol A dicyanate and **4a**, bearing the backbone shortest chain length. Not only this, but that as temperature increases the miscibility increases, unlike the results for the longer alkylene ether chains, which apparently become less miscible with bisphenol A dicyanate as temperature increases. Fig. 10 shows the results of BLENDS calculations to show the Gibbs' free energy of mixing for bisphenol A dicyanate with the other dicyanates as each undergoes polymerisation to the same extent (*i.e.* the mixing of similarly-sized cyanate oligomers is examined). The data suggest some significant changes in miscibility – notably in the case of the cyclotrimer of **4a**, which initially shows the poorest compatibility with the corresponding cyclotrimer of bisphenol A dicyanate, although the formation of the pentamer (depicted in Fig. 3) heralds a significant improvement in miscibility for practically all the dicyanate species studied here. Fig. 11 shows the results of BLENDS calculations to show the Gibbs' free energy of mixing for bisphenol A dicyanate with other species (*e.g.* monomers, trimers and pentamers of each of the alkylene ether dicyanates) that participate in the polymerisation reaction. Thus, bisphenol A dicyanate is least compatible with the cyclotrimer of **4a**, for which

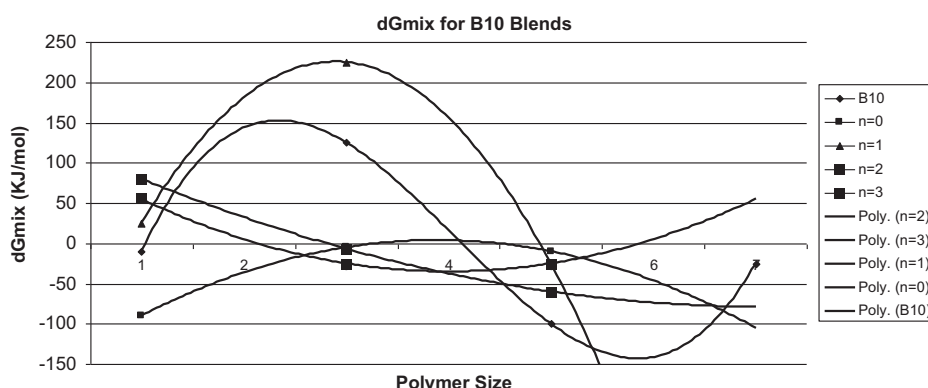


Fig. 10. Effect of oligomer size (monomer → heptamer) on miscibility with like sized bisphenol A dicyanate (B10) species.

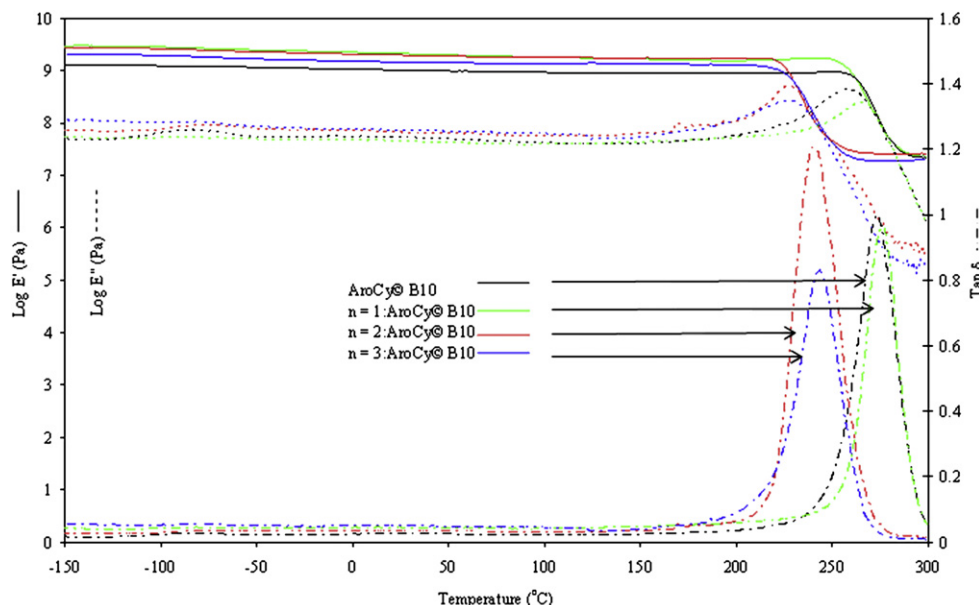


Fig. 12. DMTA for homopolymer of bisphenol A dicyanate (AroCy B10) and selected blends with alkylene ether dicyanates, $n = 1$ (**4a**), $n = 2$ (**4b**), $n = 3$ (**4c**).

a high value of ΔG_{mix} ($+225 \text{ kJ mol}^{-1}$) is calculated, whereas negative values ΔG_{mix} (ca. -15 to -25 kJ mol^{-1}) are obtained for **4b** and **4c**. Of the monomers, **4c** (containing the longest alkylene ether backbone) is seen to be the least compatible with bisphenol A dicyanate. In all cases, the pentamers are seen to be the species that are the most compatible with bisphenol A dicyanate as negative values ΔG_{mix} are calculated for all, but most negative for **4b**.

3.8. Dynamic mechanical thermal analysis of selected polycyanurate blends

A series of blends were prepared, comprising bisphenol A dicyanate and co-monomers **4a–c**, and cured prior to undertaking thermo-mechanical analysis using DMTA. The data are shown in Fig. 12 from which it is apparent that the cured neat resin blends appear well mixed and homogenous copolymer with no apparent phase separation indicated from the $\tan \delta$ profiles (as evidenced by single step transitions in the loss modulus data and single α transition peaks for each copolymer). As expected the DMTA data confirm that the storage modulus (E') of bisphenol A dicyanate (B10) is affected to differing extents by the addition of the alkylene ether dicyanates

4a + B10, $E' = 1.02 \text{ GPa}$ at 25°C , 0.98 GPa at 50°C and 0.88 GPa at 200°C

4b + B10, $E' = 2.01 \text{ GPa}$ at 25°C , 1.92 GPa at 50°C and 1.73 GPa at 200°C

4c + B10, $E' = 1.47 \text{ GPa}$ at 25°C , 1.43 GPa at 50°C and 1.31 GPa at 200°C .

Although the storage moduli at 25°C for the binary blends are significantly lower than the respective homopolymers [5], the reduction in E' over the temperature range 25 – 200°C has significantly improved compared with bisphenol A polycyanurate (0.56 GPa). For example, the introduction of **4b** appears to improve this by a factor of ca. 2, while **4a** and **4c** improve it by a factor of ca.

4. Considering the T_g values of the homopolymers are relatively low, 139°C **4b** and 121°C **4c**, this addition does not apparently affect the T_g of bisphenol A polycyanurate significantly when blended to form a copolymer (at this level of incorporation), giving values of 241°C and 247°C respectively.

4. Conclusions

The solubility parameters that were calculated for the dicyanates and corresponding oligomeric cyanurates for a commercial dicyanate monomer (based on bisphenol A) and a homologous series of dicyanates containing an alkylene ether backbone showed significant differences when using Small's and Hoy's methods, despite being based on similar structural elements. Consequently, the BLENDS module of Cerius² was used to determine the Gibbs free energy of mixing (ΔG_{mix}) values for the different monomers and for selected oligomeric species found within the binary blend during the early stages of polymerisation. In order for the simulation to be as representative as possible, the data from a published quantitative empirical study (using HPLC and MS) were used to determine the typical composition of a growing polycyanurate at selected degrees of conversion. The BLENDS module is able to rank the compatibility of different monomers (containing backbones of differing polarity) and also to distinguish between the different oligomeric species within the growing network. Thus, the initial step, the rapid formation of a cyclotrimer, produces a species that is significantly less compatible with all monomers (regardless of backbone), but the subsequent oligomerisation to form pentamer markedly improves the compatibility of the binary blend along with subsequent steps to higher polymeric forms. This is in agreement with the results of the other two more traditional measures of blend compatibility (i.e. the methods of Small and Fedors). Of course, this is a thermosetting polymer system and so the early stages of reaction, prior to gelation, when the reaction is largely chemically rather than diffusion controlled, are the most significant for our study. Once gelation commences then the ability to undergo translational movement is greatly reduced and the miscibility has a greater influence in determining e.g. phase separation and the ultimate morphology. The latest advances in our simulation work have significantly increased the size and sophistication of the models

that we can build and interrogate and work will continue to apply the results of this study to improve our understanding of phase separation behaviour.

References

- [1] Hamerton I. In: Hamerton I, editor. Chemistry and technology of cyanate esters. Glasgow: Blackie; 1994 [Chapter 1], pp. 1–6.
- [2] Weirauch KK. Proceedings of the IPC September 1975 Meeting, Chicago, USA, paper no. TP-066; 1975.
- [3] Speak SC, Sitt H, Fuse RH. 36th Int SAMPE Symp, 36, 336; 1991.
- [4] Sweetman E. Proceedings of the 1st International Conference on Multichip Modules (sponsored by ISHM and IEPS); 1992, p. 401.
- [5] Hamerton I, Howlin BJ, Klewpatinond P, Takeda S. *Macromolecules* 2009;42:7718.
- [6] Hamerton I, Howlin BJ, Klewpatinond P, Shortley HJ, Takeda S. *Polymer* 2006;47:690.
- [7] Hamerton I, Howlin BJ, Klewpatinond P, Takeda S. *Polymer* 2002;43:4599.
- [8] Davies JMR, Hamerton I, Jones JR, Povey DC, Barton JM. *J Cryst Spec Res* 1990;20:285.
- [9] Rappé AK, Goddard III WA. *J Phys Chem* 1991;95:3358.
- [10] Mayo SL, Olafson BD, Goddard III WA. *J Phys Chem* 1990;94:8897.
- [11] Allington RD, Attwood D, Hamerton I, Hay JN, Howlin BJ. *Comput Theor Polym Sci* 2001;11:467.
- [12] Bauer M, Bauer J. In: Hamerton I, editor. Chemistry and technology of cyanate esters. Glasgow: Blackie; 1994 [Chapter 3], pp. 58–86.
- [13] Hamerton I, Emsley AM, Howlin BJ, Klewpatinond P, Takeda S. *Polymer* 2003;44:4839.
- [14] Bauer M, Bauer J, Jähig S. *Macromol Chem, Macromol Symp* 1991;45:97.
- [15] Klewpatinond P. PhD Thesis, University; 2005.
- [16] Takeda S, Akiyama H, Kakiuchi H. *J Appl Polym Sci* 1988;35:1341.
- [17] Fedors RF. *Polym Eng Sci* 1974;14:147.
- [18] Hoy JJ. *Paint Technol* 1970;42:76.
- [19] Small PA. *J Appl Chem* 1953;3:71.
- [20] Cowie JMG. The chemistry and physics of modern materials. 2nd ed. Glasgow: Blackie Academic and Professional; 1991. pp. 178–9.
- [21] Rubber handbook: solubility parameters of organic compounds C-732-733. Boca Raton, Florida: CRC Press Inc.; 1979.
- [22] Fang T, Shimp DA. *Prog Polym Sci* 1995;20:61.
- [23] Kasehagen LJ, Macosko CW. *Polym Int* 1997;44:237.
- [24] Hamerton I, Heald CR, Howlin BJ. *J Mater Chem* 1996;6:311.
- [25] Bauer M, Uhlig C, Bauer J, Harris S, Dixon D. In: Side reactions during polycyclotrimerisation of cyanates and their influence on network structure and properties, synthetic versus biological networks: papers presented at polymer networks 98, the 14th polymer networks group international conference, held at the Norwegian University of Science and Technology (NTNU) in Trondheim from 28 June–3 July 1998, vol. 2. Wiley Polymer Networks Group Review Series; 1999. p. 271.
- [26] Shimp DA. Improved chromatographic resolution of dicyanate oligomers: network-building implications, Abstracts of the papers of the ACS; 1994, 208: 440–PMSE Part 2 Aug 21; 1994.
- [27] Cerius² property prediction user's reference manual, Molecular Simulations, Inc., pp. 38–51.
- [28] Patnaik SS, Pachter R. *Polymer* 2002;43:415.